$E2$ transition probabilities in ^{114}Te: A conundrum

O. Möller, N. Warr, J. Jolie, A. Dewald, A. Fitzler, A. Linnemann, and K. O. Zell
Institut für Kernphysik, Universtät zu Köln, Zülpicher Straße 77, D-50937 Köln, Germany

P. E. Garrett*
Lawrence Livermore National Laboratory, Livermore, California 94551, USA

S. W. Yates
University of Kentucky, Lexington, Kentucky 40506-0055, USA
(Received 11 February 2005; published 30 June 2005)

Lifetimes in ^{114}Te were determined using the recoil distance Doppler-shift technique with a plunger device coupled to five HP Ge detectors enhanced by one Euroball cluster detector. The experiment was carried out at the Cologne FN Tandem facility using the ^{93}Nb(^{24}Mg,$p2n$) reaction at 90 MeV. The differential decay curve method in coincidence mode was employed to derive lifetimes for seven excited states, whereas the lifetime of an isomeric state was obtained in singles mode. The resulting $E2$ transition probabilities are shown to be very anomalous in comparison with the vibrational energy spacings of the ground-state band.

DOI: 10.1103/PhysRevC.71.064324 PACS number(s): 21.10.Tg, 23.20.−g, 27.60.+j

I. INTRODUCTION

In recent years the nucleus ^{110}Cd has been intensively studied and has been shown to be a very good example of an anharmonic vibrator [1,2]. This nucleus exhibits, in addition to the spherical phonon states, a shape coexistence structure because of $4h$-$2p$ excitations across the $Z = 50$ shell, which can be described as intruder states [3]. In the context of particle-hole invariance formulated in terms of intruder spin [4,5], ^{114}Te can be expected to show an excitation pattern similar to that of ^{110}Cd, but based on $2p$ excitations instead of $2h$ ones, may thus also exhibit a level structure characteristic of the $U(5)$ dynamical symmetry.

As mentioned in the systematic study of Ref. [6], there are four criteria to be satisfied if a nucleus is vibrational: (i) a ratio $R_{4/2}$ equal to 2, (ii) a nearly degenerate two-phonon triplet, (iii) level energies following the analytical expression for the $U(5)$ limit of the Interacting Boson Model (IBM), and (iv) collective electric-quadrupole transitions between states differing by one phonon and strong hinderance of $E2$ transition between states differing by more than one phonon. Despite the $R_{4/2}$ ratio of 2.09, Ref. [6] did not include ^{114}Te with the good vibrational nuclei because of the lack of experimental data [7]. According to the present work, it seems that this nucleus mimics the $U(5)$ dynamical symmetry not only because the ratio $R_{4/2}$ is near to the harmonic value of 2 but also because it fullfills three of the four criteria. Nevertheless, as shown, the last criterion on the absolute transition rates is badly violated.

Unlike ^{110}Cd, ^{114}Te has not been extensively studied. Only a few experimental studies have been reported, and no absolute transition rates are known. ^{114}Te was previously studied by only a few reactions and, notably, knowledge of the low-spin structure of ^{114}Te was lacking. The results are compiled in Ref. [8]; however, we should mention the work of Lönnroth *et al*. [9] and their study of the ^{114}Sn(^{3}He,$n\gamma$)^{114}Te reaction, Zimmerman's [10] study from ^{114}I β decay, Moon *et al*. [11] using the ^{89}Y(^{28}Si,$p2n$) and ^{89}Y(^{29}Si,$p3n$) reactions, and Janzen's [12] study with the ^{94}Mo(^{23}Na,$p2n\gamma$)^{114}Te reaction.

With the aim of elucidating the structure of ^{114}Te and testing the validity of vibrational structure for this nucleus, a lifetime measurement was performed using a ^{24}Mg beam accelerated with the FN Tandem at the University of Cologne. The experiment is described in Sec. II. The analysis of the experiment is presented in Sec. III. The last section presents the comparison of our results with theory.

II. PERFORMED EXPERIMENT

A recoil distance Doppler-shift (RDDS) experiment was performed with the Köln coincidence plunger device at the FN Tandem facility at the University of Cologne. Excited states of ^{114}Te were populated using the ^{93}Nb(^{24}Mg,$p2n$) reaction at a beam energy of 90 MeV. The calculated cross section in the ($p2n$)-channel was 100 mb. The target was a 1.1 mg/cm^2 self-supporting foil of natural Nb. A 6 mg/cm^2 gold foil stopped the recoiling nuclei, which had an average velocity of $v/c = 1.36\%$. The setup (Fig. 1) consisted of one Euroball cluster detector [13,14] at 0° relative to the beam axis and five large volume HP Ge detectors at polar angles of 143°. All detectors were positioned very close (≈11 cm) to the target, increasing the total photopeak efficiency of this setup to about 2.4% at 1.3 MeV.

The detectors can be grouped into two angular rings—the five detectors in the backward direction ($\theta_0 = 143°$, *ring* 0) and the six outer segments ($\theta_1 = 34°$, *ring* 1) of the Euroball cluster detector. Both combinations between these two rings were used for analysis. Spectra received from the inner cluster segment were used only to determine the recoil velocity, taking advantage of the maximum Doppler shift at $\theta_2 = 0°$.

*Present address: Department of Physics, University of Guelph, Guelph Ontario N1G2W1, Canada.

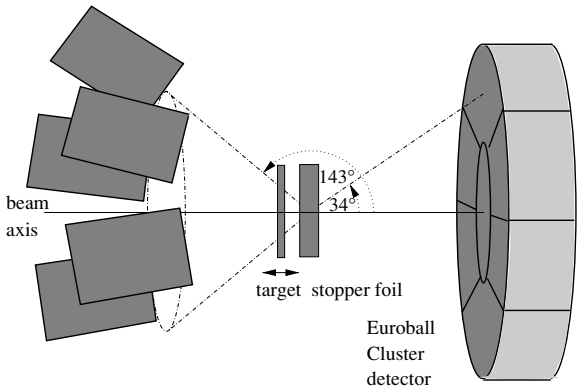

FIG. 1. Schematic drawing of the experimental setup.

Coincidence data were collected for 13 different target-to-stopper distances x, between 4 and 3000 μm. A total of 2.7×10^9 $\gamma\gamma$ coincidence events were collected and sorted into $13 \times 8 = 104$ 4k $\times$ 4k $\gamma\gamma$ matrices $M_{ij}(x)$, corresponding to eight possible pairwise combinations of the two detector rings and the single inner cluster segment. Figures 2 and 3 show the three lowest transitions of the ground-state band of ^{114}Te in gated-coincidence spectra, illustrating the quality of the data. The spectra shown were obtained from ring 1, by gating on ring 0. The partial level scheme of ^{114}Te in Fig. 4 shows the states observed in the present experiment.

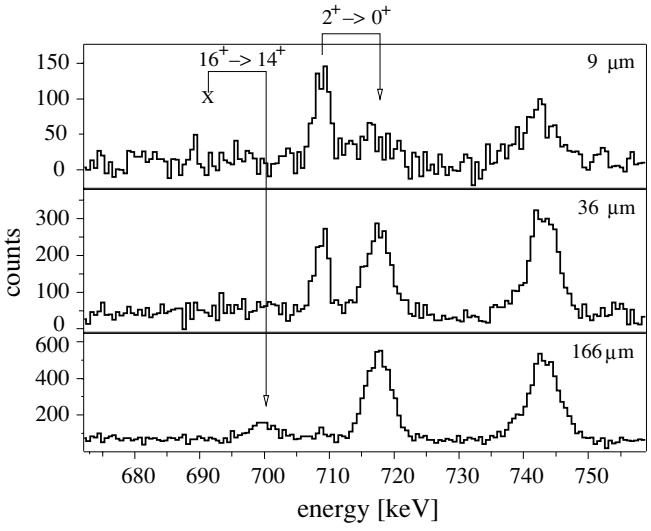

FIG. 2. Coincidence spectra resulting from gating on the $4^+ \rightarrow 2^+$ shifted component observed in detector-ring 1. Indicated is the $2^+ \rightarrow 0^+$ transition used to determine the 2^+ lifetime. In these spectra the shifted component lies higher in energy ($\theta_1 = 34^\circ$) than the unshifted component. The position labeled X indicates where the unshifted component of a transition above the gating transition would be; it cannot be observed because of gating on the shifted component of a lower lying transition.

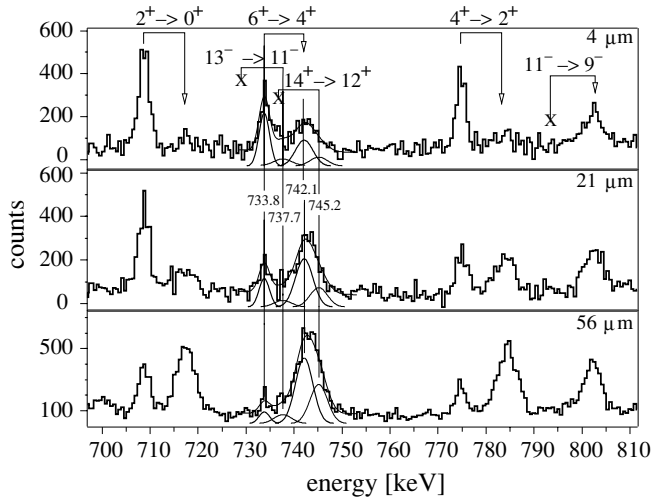

FIG. 3. Coincidence spectra resulting from gating on the $8^+ \rightarrow 6^+$ shifted component observed in detector-ring 1. The labeling is as described in the legend to Fig. 2. The fits of the peak components from the $6^+ \rightarrow 4^+$ transition, as well as contaminants that had to be taken into account, are shown.

III. ANALYSIS AND RESULTS

To determine lifetimes, the differential decay curve (DDC) method [15] was used in the coincidence mode, thus avoiding all problems related to the feeding history of the state of interest, especially the problem of unobserved side feeding.

From the spectra generated by gating on the shifted components of feeding γ transitions, one obtains the peak intensities of γ transitions depopulating the level of interest at different target-to-stopper distances x. The data of different target-stopper separations x have to be normalized to the corresponding number of ^{114}Te nuclei produced at each separation x. In practice this was done by first generating spectra with gates set on both the shifted and unshifted components of the $6^+ \rightarrow 4^+$ transition. In a second step the summed intensities of the shifted and unshifted components of the higher lying transitions $8^+ \rightarrow 6^+$ and $10^+ \rightarrow 8^+$ were determined. For each set of matrices $M_{ij}(x)$ these intensities are proportional to the number of ^{114}Te nuclei produced at the corresponding distance x and thus can be used as normalization factors. In this way four independent sets were derived and checked for consistency. In the same way additional sets of normalization factors were determined by using the $4^+ \rightarrow 2^+$ and $2^+ \rightarrow 0^+$ transitions for gating and the intensities of higher lying transitions. In particular, normalization factors derived from the spectra gated on the $2^+ \rightarrow 0^+$ transition might be affected by the deorientation effect. Actually the deorientation effect was not observed. This is caused by the intensive slow feeding of the ground-state band and the detector angles of 34° and 143°, which are close to 55° and 125° where the P_2 of angular distributions is zero. As final normalization factors the averages of the independent sets of normalization factors were adopted.

In our notation the abbreviations s or u stand for "shifted" or "unshifted" component of a given γ transition denoted by a capital index. The DDC method gives the lifetime $\tau(x)$ of

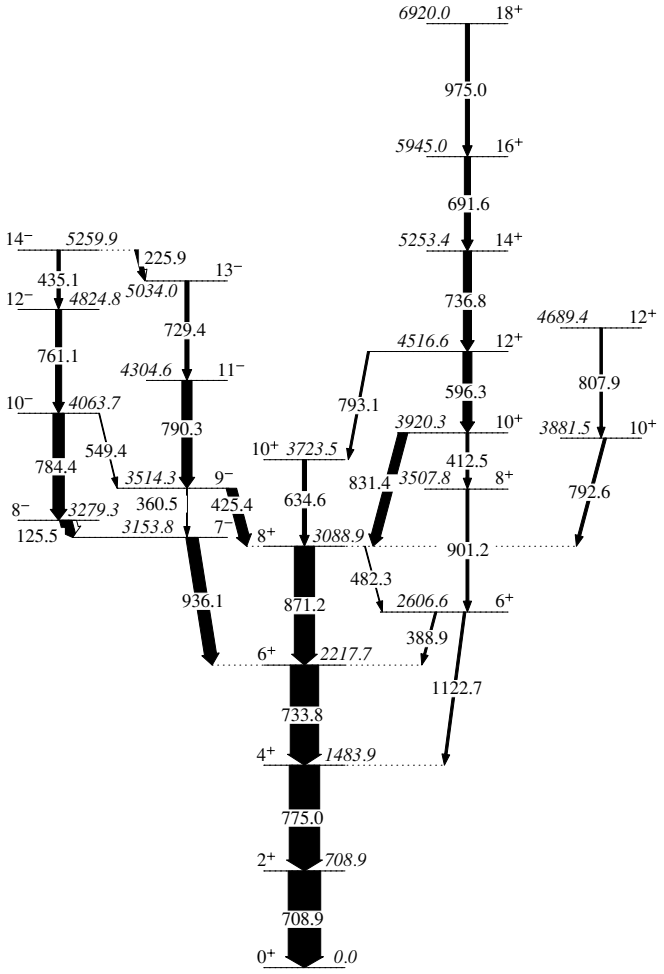

FIG. 4. Partial level scheme of ^{114}Te with transitions observed in the (^{24}Mg,$p2n$) reaction. The assignments of levels to bands are taken from Ref. [11].

a state in the special case of gating on the Doppler-shifted component of a direct feeding transition as follows:

$$\tau(x) = \frac{I_{\mathrm{su}}^{\mathrm{BA}}(x)}{v \cdot \frac{d}{dx} I_{\mathrm{ss}}^{\mathrm{BA}}(x)}, \qquad (1)$$

where v denotes the recoil velocity. The quantities $I_{\mathrm{su}}^{\mathrm{BA}}(x)$ and $I_{\mathrm{ss}}^{\mathrm{BA}}(x)$ denote the normalized, measured intensities of the depopulating γ transition A in coincidence with the shifted component of a populating γ transition B.

The derivative, $(d/dx)I_{\mathrm{ss}}^{\mathrm{BA}}(x)$, was determined by fitting piecewise continuously differentiable second-order polynomials to the intensity values $I_{\mathrm{su}}^{\mathrm{BA}}(x)$. Because the lifetime τ is the constant of proportionality between unshifted and the derivative of Doppler-shifted intensity, deviations from a constant emphasize systematic errors. The statistics of the data defines the so-called region of sensitivity, and only τ values obtained within this region were used to determine the resulting lifetime. The analysis involved is illustrated in Fig. 5, a detailed description of this method and the derivation of Eq. (1) can be found in Refs. [15,16].

For the lifetime analysis of low-spin states in the ground-state band of ^{114}Te with the reaction used, one has to deal

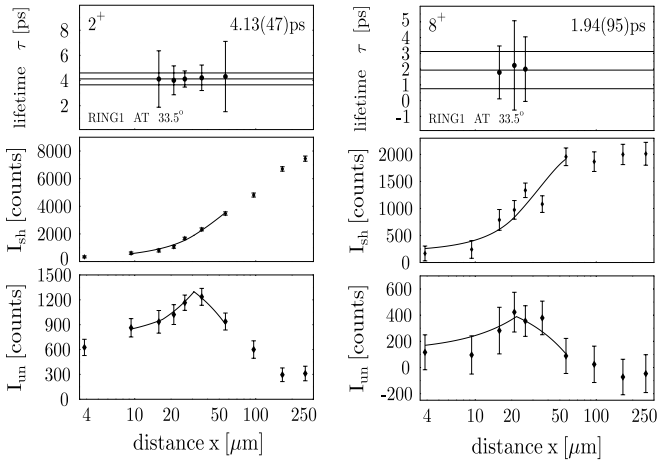

FIG. 5. Determination of the lifetime of the 2^+ (left panels) and 8^+ (right panels) states measured with the detectors at 33.5°. The bottom frame displays the denominator in Eq. (1), whereas the numerator is displayed in the middle frame. The continuous curve in the bottom frame represents the fitted derivative of Doppler-shifted intensity (multiplied by the lifetime τ) as a function of the target-to-stopper distance.

with the problem that 90% of the feeding of the ground-state band is from long-lived states. The 6^+ level of the ground-state band is populated indirectly from a 8^- state at 3279 keV (τ = 940 ps), whereas the 8^+ state is fed from a 9^- level at 3514 keV and a 10^+ level at 3920 keV with lifetimes of 43 and 34 ps, respectively. All these lifetimes were measured for the first time in this work.

Figure 6 illustrates the ground-state band feeding. Figure 7 shows spectra measured at different target-to-stopper distances; the feeding transitions and their Doppler-shifted components are indicated. The left panel shows spectra obtained with the detectors at forward angles, and the middle and right panels with the detectors at backward angles with respect to the beam axis. At a distance of 250 μm, which corresponds to a time of flight of 61 ps of the recoiling nuclei, two-thirds of the

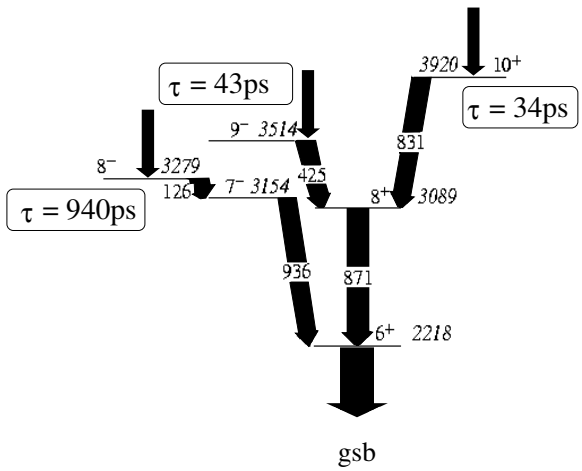

FIG. 6. Partial level scheme showing the main feeding transitions into the ground-state band (gsb) arise from isomeric levels.

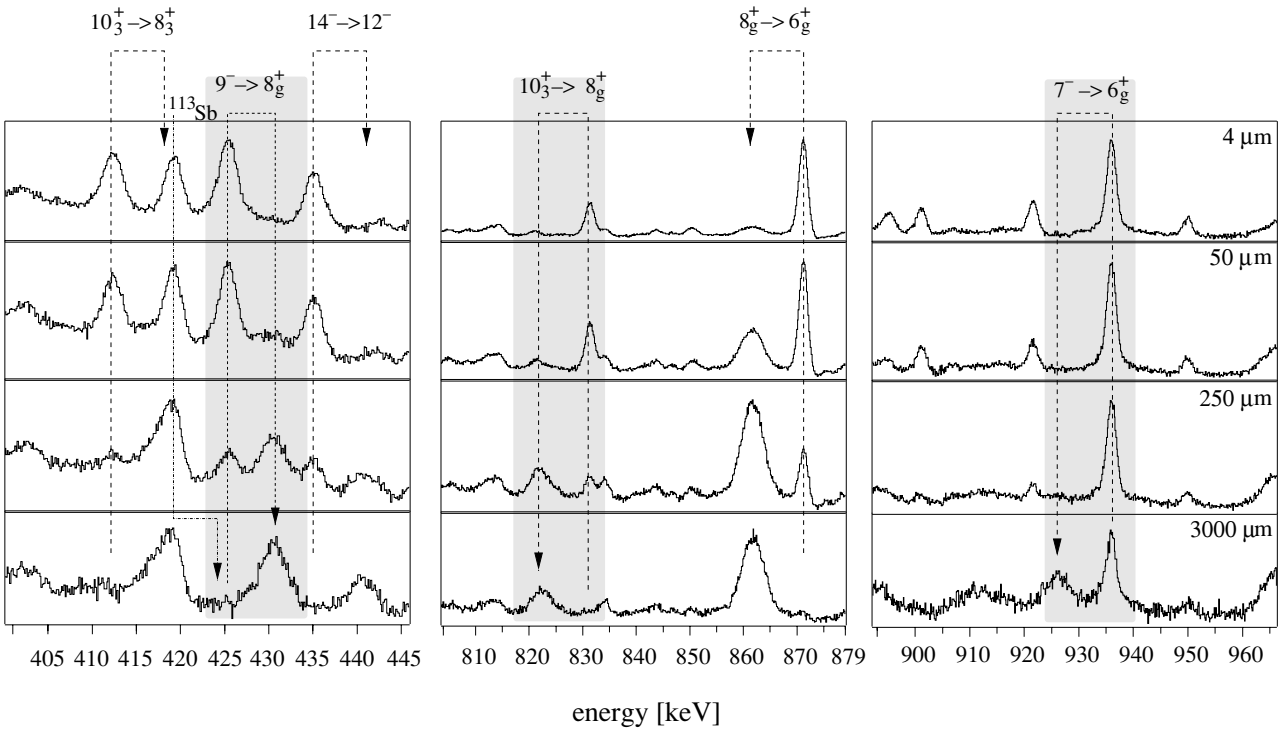

FIG. 7. γ-Ray singles spectra showing the slow feeding of the ground-state band for four target-to-stopper distances. The spectra were obtained at 33° (left panel) or 142° (middle and right panels), respectively. The three main feeders of the gsb are shown against shadowed background, also indicated is a decay of a known isomer in ^{113}Sb ($\tau \approx 5$ ns) at 419 keV and three other transitions in ^{114}Te. To draw attention to the relative shifts in intensity, no scale is given on the y axis.

total γ-ray intensity of the 425-keV transition, which decays from the 9^- level with a lifetime of $\tau = 43$ ps, appears in the Doppler-shifted component. For comparision, a 419-keV peak is indicated that depopulates a known isomer in ^{113}Sb with a lifetime of 5.3 ns [17] and almost no Doppler-shifted intensity can be found even at a target-to-stopper distance of 3000 μm. The ratio of Doppler-shifted and unshifted intensity of the two peaks at 412 and 831 keV, corresponding to the $10_3^+ \rightarrow 8_2^+$ and $10_3^+ \rightarrow 8_1^+$ transitions, respectively, is, as expected, the same in terms of the target-to-stopper distances. The longest feeding time into the ground-state band originates from the 936-keV transition ($\tau_{\text{eff}} = 940$ ps). After a flight distance of 3000 μm, corresponding to a time of flight of 735 ps, a considerable fraction of nuclei still decay after being stopped. In contrast to this slow feeding, the expected lifetimes of the low-spin states in the ground-state band are of the order of a few ps. A slow feeding of a short-lived state always generates a problem for determination of the short lifetime. Nevertheless, sufficient statistics were collected in coincidence mode to allow gating on the shifted component of the feeding transition and, using the DDC method, eliminated the problem of the feeding history.

For the lifetime analysis of the 4_1^+ and 12_1^+ states, contaminant lines belonging to the same cascade in ^{114}Te forced the use of a small gate width in one ring and eliminated the use of the other ring for the gating condition. Consequently the statistics of the resulting gated spectra were reduced considerably. Table I gives details on the detector rings used for gating and the considered contaminant lines.

In order to find clean gates in these two cases, we simulated the relevant part of the spectrum by using Gaussians for the shifted and unshifted components of the known transitions. The positions of the shifted components were fixed by using the Doppler formula and the experimentally determined mean recoil velocity. The widths of both the unshifted and shifted components were obtained from a width calibration, gained from the widths of uncontaminated peaks at different energies. As demonstrated in Fig. 8, only a narrow gate could be placed on the high-velocity tail (the spectrum was simulated for a detector at the backward angle) of the shifted component of

TABLE I. List of gates and detector rings used to produce gated spectra. Index SH / UN denotes gate on shifted / unshifted component of a given transition energy.

E_x (keV)	E_γ (keV)	E^{gate} (keV)	Det. Ring	Contaminants
708.9	708.9	775^{SH}	0	$10^- \longrightarrow 8^-$; 784.4 keV
1483.9	775.0	733.8^{SH}	1	$14^+ \longrightarrow 12^+$; 736.8 keV
				$13^- \longrightarrow 11^-$; 729.4 keV
2217.7	733.8	871.2^{SH}	0,1	
3088.9	871.2	831.4^{SH}	0,1	
3514.3	425.4	790.3^{SH}	0,1	
3920.3	831.4	596.3^{SH}	0,1	
4516.6	596.3	736.8^{SH}	1	$6^+ \longrightarrow 4^+$; 733.8 keV
3279.3	125.5	708.9^{UN}	0,1	

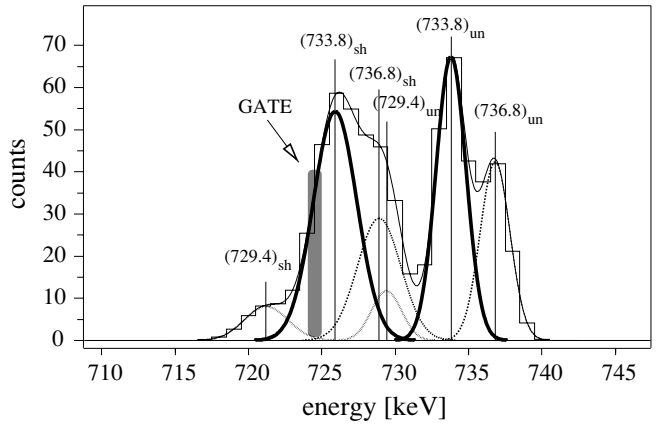

FIG. 8. Simulated spectrum of widths-calibrated Gaussians in the 740-keV region showing the $6^+_{gsb} \rightarrow 4^+_{gsb}$ transition, its contamining peaks as well as their Doppler-shifted components, for a detector at the backward angle of 143°. Because the gate on the shifted component is asymmetric relative to its centroid, recoils with higher velocities than the mean v/c are selected. This procedure makes it necessary to correct the lifetime resulting from spectra received from this gate.

the feeding transition of the 4^+ state. In the resulting spectra produced by gating on a clean shifted component, no shifted components of transitions lying higher in the cascade can be seen. This fact provides a sensitive check for remaining contaminant lines. From Fig. 9 it becomes evident that, despite

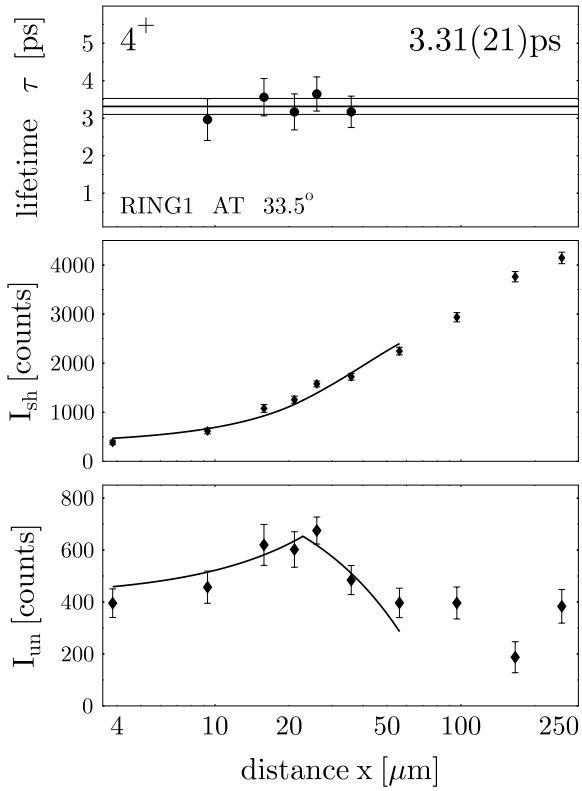

FIG. 9. Determination of the lifetime of the 4^+ state measured with detectors at 33.5°.

rather poor statistics, it is still possible to deduce a clear signal for lifetime analysis.

In the case of the 4^+_1 and 12^+_1 levels, the lifetimes were analyzed in a first step by applying the standard differential decay curve method (DDCM) and using the mean recoil velocity. In a second step, the lifetime had to be corrected for the specific velocity, because the asymmetric gating conditions select a higher, or lower, velocity than the mean recoil velocity. To determine the actual recoil velocity for the gates used, the flight peak was deconvoluted with a Gaussian representing the detector resolution. The Gaussian obtained was transferred into a velocity distribution to assign the specific velocity for every single channel of the flight component. From the ratio of the resulting selected velocity component and the mean velocity, correction factors of 0.93 and 0.87 for the 4^+_1 and the 12^+_1 level respectively, were extracted.

In Fig. 5 the τ curves of the 2^+ and the 8^+ states are given. In all cases lifetimes were determined from spectra obtained by gating on the direct feeding transition except in the case of the 8^- isomeric state. Intensities of depopulating transitions of the states of interest were determined in the resulting gated spectra in both detector-rings 0 and 1. For the lifetime analysis of the isomeric state, a different technique was used and spectra were created by gating on the unshifted component of the $2^+_1 \longrightarrow 0^+_1$ transition. In these spectra we determined decay curves for the unshifted component of both feeding and depopulating transitions, and the lifetime was deduced in the same way as in an analysis of singles spectra.

In total, eight level lifetimes could be extracted from the RDDS experiment. Table II lists the resulting lifetimes obtained from the experiment, and the deduced $B(E2)$ values for the ground-state band.

IV. DISCUSSION

In this section, we compare our results to the IBM, which describes the valence nucleon pairs as s and d bosons. The comparison will be restricted to the vibrational structures, because no clear candidate for the band head of the intruder band was identified. Finally, we compare our results with the one-broken-pair model, which allows one of the nucleon pairs to be broken, and the QPM, which explicitly constructs phonons from two-quasiparticles components.

A. Ground-state band structure

To establish the vibrational character of a nucleus, we rely partially on the selection criteria presented in Ref. [6]. The first criterion is that the ratio $R_{4/2} = 2.09$ is nearly equal to 2. This criterion can be extended to higher members of the ground-state band; one finds that $R_{6/2} = 3.17$ and $R_{8/2} = 4.36$. These nearly harmonic values should be compared to those in ^{110}Cd, where $R_{4/2} = 2.34$, $R_{6/2} = 3.77$, and $R_{8/2} = 4.98$. The agreement can be extended when prolonging the band with the 3881.5 keV $L = 10^+$ and 4689.4 $L = 12^+$ states. The second criterion concerns the energy spread S (as defined in Ref. [6]) between the upper and lower members of the two-phonon states. If one considers the 1348.1 keV $L = (0^+)$ and the

TABLE II. Adopted lifetimes τ_{exp}, branching ratios br, $B(E2)$, and Q_t values of analyzed transitions in ^{114}Te. Branchings are taken from Ref. [8], except those denoted by Ref. (2), which were determined from our data. The transition denoted by Ref. (1) was not observed in the present experiment.

E_x (keV)	J_i^π	E_γ (keV)	br %	τ_{exp} (ps)	$B(E2)$ ($W.u.$)	Q_t (eb)
708.9	2_1^+	708.9	100	4.09(33)	34.0(30)	2.36(10)
1483.9	4_1^+	775.0	100	3.11(30)	28.7(30)	1.81(9)
2217.7	6_1^+	733.8	100	2.74(50)	42.7(80)	2.11(20)
3088.9	8_1^+	871.2	100	1.88(65)	25.1(90)	1.58(30)
3514.3	9_1^-	425.4	79(8)	43.0(40)	0.10(2) (E1)	
		233.9	21(4)	43.0(40)	0.011(3) (M1)	
3920.3	10_3^+	831.4	50(5)	33.7(20)	0.93(11)	0.30(2)
		411.9	36(5)	33.7(20)	21.6(43)	1.45(15)
		196.4 [1]	14(2)			
4516.6	12_1^+	596.3	70(10) [2]	4.2(8)	54.2(128)	2.27(27)
		793.1	30(10) [2]	4.2(8)	5.60(214)	0.73(14)
3279.3	8_1^-	125.5	100	940(150)		

1391.3 keV $L = 2^+$ states [8] as members of this triplet, the value for ^{114}Te is $S = 137$ keV, far from the condition $S < 30$ keV [6]. However, as noted in Ref. [6], except for ^{110}Pd, all vibrational nuclei exhibit large anharmonicities in the two-phonon triplet. Based on these two criteria, it seems reasonable to try to describe ^{114}Te using the $U(5)$ dynamical symmetry. The Hamiltonian in this limit of the IBM is given by the following:

$$\hat{H} = \epsilon \hat{C}_1[U(5)] + \alpha \hat{C}_2[U(5)] + \beta \hat{C}_2[O(5)] + \gamma \hat{C}_2[O(3)]. \tag{2}$$

with $\hat{C}_n(G)$ the nth order Casimir operator of the group G. The eigenvalues of the Hamiltonian given by Eq. (3) lead to the third criterion for a good vibrational nucleus, namely that the level energies are well approximated by the formula:

$$E(U5) = \epsilon n_d + \alpha n_d(n_d + 4) + \beta \nu(\nu + 3) + \gamma L(L + 1), \tag{3}$$

where n_d is the quantum number giving the number of d bosons, ν the d-boson seniority, and L the spin. The experimental knowledge of low-spin yrare states is, however, almost non existent in ^{114}Te, so we apply Eq. (3) only to the ground-state band. For this band the states have $n_d = \nu = 2L$ and Eq. (3) reduces to the following:

$$E(L) = aL^2 + bL. \tag{4}$$

The fitted parameters give the values $a = 2.8$ keV and $b = 359$ keV. Figure 10 compares the level scheme of the proposed band structure for ^{114}Te with the data in an L versus $E(L)$ plot. Clearly visible is the nearly linear dependence, including the 6_1^+ state, which is typically too low in energy in the heavier Te isotopes, and the absence of important other distortions in the ground-state band.

Although the results are obtained using a very limited data set, one might conclude on the basis of the energies only that ^{114}Te is a nice example of a collective near-harmonic vibrator.

B. Electric quadrupole transitions

The last criterion concerns the electromagnetic transition rates which should be collective and be related by $B(E2; L \to L-2) = L \times B(E2; 2^+ \to 0^+)/2$ in the geometric collective model [18] for the states with $L = 2N_{phonon}$, and by the following:

$$B(E2; L \to L-2) = \frac{L(N+1-L/2)}{2N} B(E2; 2^+ \to 0^+) \tag{5}$$

in the $U(5)$ limit of the IBM [19] due to the limited boson number N (finite-N effect). Figure 11 compares the collective model and the IBM predictions, with $N = 7$, with the measured $B(E2)$ values. One observes a large discrepancy. None of the measured $B(E2)$ values fits even approximately the theoretical predictions. In fact, the best fit of the data would be that all $B(E2)$ values in the ground state band are constant. In comparison, ^{110}Cd has the values 27.4(3), 46(6), and 62(18)

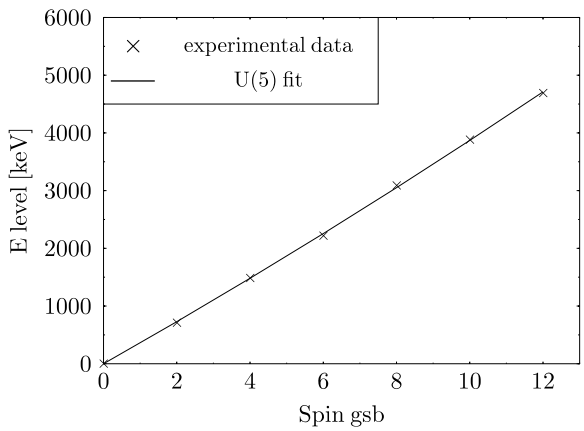

FIG. 10. Comparison between experimental (dots) and theoretical (line) excited states of the ground-state band calculated using the $U(5)$ dynamical symmetry.

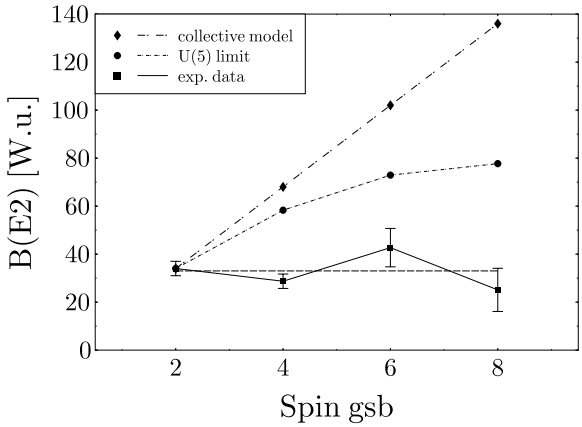

FIG. 11. Derived $B(E2)$ values in the ground-state band plotted as a function of spin. Given are the experimental values (dots), the prediction of the collective model and the IBM, and of a constant $B(E2)$ value.

(all in W.u.) for the $B(E2)$ values deexciting the 2^+, 4^+ and 6^+ states [2,20] in perfect agreement with 27.4, 47, and 59 obtained using Eq. (5). As one might wonder whether ^{114}Te is collective at all, Fig. 12 compares the $B(E2; 0^+ \rightarrow 2^+)$ value with the systematics in the whole Te-Ba region using the $N_\pi N_\nu$ scheme [21]. To compare across the neutron midshell, the rule [22]

$$B(E2; 0^+ \rightarrow 2^+) = \alpha \cdot N_\pi \dot{N}_\nu + B(E2; 0^+ \rightarrow 2^+)_{^{124}\mathrm{Sn}}, \quad (6)$$

with N_π and N_ν the number of proton and neutron bosons, is plotted with the data. The value for $N = 62$ ^{114}Te is in approximate agreement with its cross midshell partner $N = 70$ ^{122}Te, as expected. Therefore ^{114}Te exhibits an appropiate degree of collectivity—expected from systematics. Thus, the ^{114}Te level scheme exhibits a vibrational character, its $B(E2; 2^+ \rightarrow 0^+)$ value indicates that it is collectively enhanced, yet the B(E2) values in the ground-state band are approximately constant,

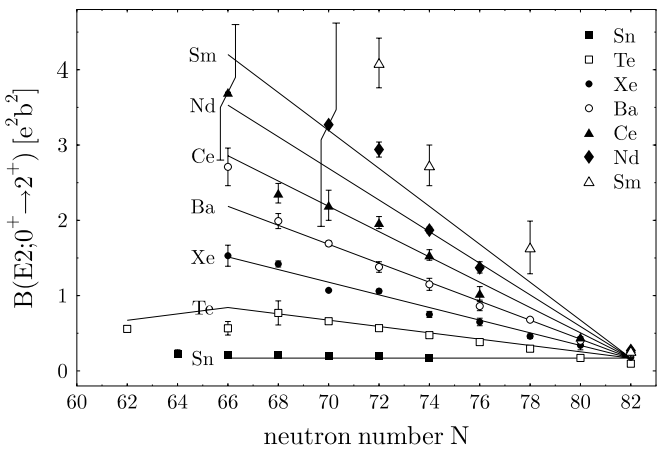

FIG. 12. Comparison of the $B(E2; 0_1^+ \rightarrow 2_1^+)$ to the predictions of Eq. (6) using the value $\alpha = 0.0215\ e^2b^2$ from Ref. [22].

contrary to a vibrational structure. This observation together with a similar one in ^{98}Ru [23] have led to a systematic search for nuclei having $B(E2; 4_1^+ \rightarrow 2_1^+)$ values smaller than their $B(E2; 2_1^+ \rightarrow 0_1^+)$ value [24]. Other nuclei in the $Z = 40-80$ mass region were identified, including the nearby isobar ^{114}Xe where the $B(E2)$ values were also measured using the DDCM [25]. No reasonable explanation was found.

C. Other approaches

Strange decay patterns for the higher spin states in the ground-state band have already been discussed for other Tellurium isotopes and more particularly for ^{118}Te and ^{120}Te [26]. There they could be explained by the presence of a broken-pair component in the states of interest. But for these non collective 8^+ and 10^+ states, the one-broken-pair calculation is not in accordance with the experiment as it does not give low-lying states. Indeed, the calculated excitation energies for these states give 4.64 and 4.81 MeV for 8^+ and 4.67 and 4.83 MeV for 10^+, respectively, which are completely in disagreement with the experimental energies observed in ^{114}Te.

Recently, the quasiparticle phonon model (QPM) has been applied to the theoretical description of ^{114}Te. Using this description, Grinberg *et al.* [27] obtained excitation energies of 3.35 and 3.45 MeV for the two lowest 8^+ states and of 3.58 and 3.92 MeV for the first 10^+, in reasonable agreement with the states shown in Fig. 1. They find, however, a collective four-phonon character for the first excited 8^+ state. Unfortunately, they do not give theoretical $B(E2)$ values, making it hard to judge the degree of collectivity predicted by the QPM.

V. CONCLUSIONS

For the first time, lifetimes of excited states in ^{114}Te have been measured. Although the energy spectrum of ^{114}Te is very well described by a slightly anharmonic vibrator, the obtained $B(E2)$ values are in strong contradiction with the theoretical predictions of the $U(5)$ limit of the interacting boson model. In fact, we are not aware of any model that can explain the data. Interestingly, our observation is not unique and other abnormal cases have been recently identified [24].

ACKNOWLEDGMENTS

The authors acknowledge many discussions with R. B. Cakirli and R. F. Casten on anomalous $B(E2)$ values. Work performed in part under the auspices of the US Department of Energy by University of California Lawrence Livermore National Laboratory under contract no. W-7405-ENG-48. This material is also based on work supported by the U.S. National Science Foundation under Grant PHY-0354656.

[1] F. Corminboeuf, T. B. Brown, L. Genilloud, C. D. Hannant, J. Jolie, J. Kern, N. Warr, and S. W. Yates, Phys. Rev. Lett. **84**, 4060 (2000).
[2] F. Corminboeuf, T. B. Brown, L. Genilloud, C. D. Hannant, J. Jolie, J. Kern, N. Warr, and S. W. Yates, Phys. Rev. C **63**, 014305 (2000).
[3] K. Heyde, P. Van Isacker, M. Waroquier, G. Wenes, and M. Sambataro, Phys. Rev. C **25**, 3160 (1982).
[4] K. Heyde, C. De Coster, J. Jolie, and J. L. Wood, Phys. Rev. C **46**, 541 (1992).
[5] H. Lehmann, J. Jolie, C. De Coster, B. Decroix, K. Heyde, and J. L. Wood, Nucl. Phys. **A621**, 767 (1997).
[6] J. Kern, P. E. Garrett, J. Jolie, and H. Lehmann, Nucl. Phys. **A593**, 21 (1995).
[7] J. Kern (private communication).
[8] J. Blachot, Nucl. Data Sheets **97**, 593 (2002).
[9] T. Lönnroth, A. Virtanen, and J. Hattula, Phys. Scr. **34**, 682 (1986).
[10] B. E. Zimmerman, Thesis, Univ. Maryland (1992).
[11] C. B. Moon, J. U. Kwon, S. J. Chae, J. C. Kim, S. H. Bhatti, C. S. Lee, T. Komatsubara, J. Mukai, T. Hayakawa, H. Kimura, J. Lu, M. Matsuda, T. Watanabe, and K. Furuno *et al*., Phys. Rev. C **51**, 2222 (1995).
[12] V. P. Janzen, Thesis, McMaster University (1985).
[13] H. G. Thomas, in *Wissenschaftliche Schriftenreihe Physik* (Verlag Dr. Köster, Berlin, 1995), Vol. 38.
[14] J. Eberth, H. G. Thomas, D. Weisshaar, F. Becker, B. Fiedler, S. Skoda, P. von Brentano, C. Gund, L. Palafox, P. Reiter, D. Schwalm, D. Habs, T. Servene, R. Schwengner, H. Schnare, W. Schulze, H. Prade, G. Winter, A. Jungclaus, C. Lingk, C. Teich, and K. P. Lieb *et al*. (Euroball Collaboration), Prog. Part. Nucl. Phys. **38**, 29 (1997).
[15] A. Dewald, S. Harissopulos, and P. von Brentano, Z. Phys. A **334**, 163 (1989).
[16] A. Dewald, P. Petkov, R. Wrzal, G. Siems, R. Wirowski, P. Sala, G. Böhm, A. Gelberg, K. O. Zell, P. von Brentano, P. J. Nolan, A. J. Kirwan, D. J. Bishop, R. Julin, A. Lampinen, and J. Hattulaet *et al*., in *Selected Topics in Nuclear Structure, Proceedings of the XXV Zakopane School on Physics*, edited by J. Styczen and Z. Stachura (World Scientific, Singapore, 1990), Vol. 2, p. 152.
[17] S.-C. Wu, Nucl. Data Sheets **91**, 1 (2000).
[18] A. Bohr and B. R. Mottelson, *Nuclear Structure* (Benjamin, New York, 1975), Vol. 2.
[19] F. Iachello and A. Arima, *The Interacting Boson Model* (Cambridge University Press, Cambridge, 1987).
[20] D. De Frenne and E. Jacobs, Nucl. Data Sheets **89**, 481 (2000).
[21] R. F. Casten, Nucl. Phys. **A443**, 1 (1985).
[22] A. Dewald, Prog. Part. Nucl. Phys. **28**, 409 (1992).
[23] R. B. Cakirli *et al*., Phys. Rev. C. **70**, 044312 (2004).
[24] R. B. Cakirli, R. F. Casten, J. Jolie, and N. Warr, Phys. Rev. C. **70**, 047302 (2004).
[25] G. de Angelis *et al*., Phys. Lett. **B535**, 93 (2002).
[26] J. J. Van Ruyven, W. H. A. Hesselink, J. Akkermans, P. Van Nes, and H. Verheul, Nucl. Phys. **A380**, 125 (1982).
[27] M. Grinberg, Ch. Protochristov, W. Andrejtscheff, G. Lo Bianco, and G. Falconi, Phys. Rev. C **61**, 024317 (2000).